

# Challenges in Brain Magnetic Resonance Image Segmentation

Roya Babaie Aghdam<sup>a</sup>, Atieh Sadat Bayat Ghiasi<sup>b</sup>, Parastoo Fatemi<sup>c</sup>, Nazanin Sadat Hashemi<sup>d\*</sup>

<sup>a,b,c,d</sup>Islamic Azad University, North Tehran Branch, Faculty of Engineering, Department of Information Technology

<sup>d</sup>Email: [nazaninhshmi@yahoo.com](mailto:nazaninhshmi@yahoo.com)

## Abstract

Over the past several decades, the application of magnetic resonance imaging (MRI) has been rapidly expanding in the areas of brain research studies and clinical diagnosis. One of the most important steps in brain MRI data preparation is the removal of unwanted brain regions, which is followed by segmentation of the brain into three main regions – white matter (WM), grey matter (GM) and cerebrospinal fluid (CSF) – or into subregions. In brain MRI analysis, image segmentation is commonly used for measuring and visualizing the brain's anatomical structures, analyzing brain changes, delineating pathological regions, and surgical planning and image-guided interventions. Brain segmentation allows clinicians and researchers to concentrate on a specific region in the brain in their analyses. However, brain segmentation is a difficult task due to high similarities and correlations of image intensity among brain regions. In this review, image segmentation algorithms used for dividing the brain into different sectors were discussed in detail. The potential for using the fuzzy c-means (FCM) unsupervised clustering algorithm and certain hybrid (combined) methods to segment brain MR images was demonstrated. Additionally, certain validation techniques that are required to demonstrate the performance of segmentation methods in terms of accuracy rates were described.

**Keywords:** Image segmentation; classification; brain imaging; MRI.

---

\* Corresponding author.

## **1. Introduction**

Medical imaging applications in clinical diagnosis and brain research studies have dramatically expanded over the past few decades. Among imaging modalities, magnetic resonance imaging (MRI) is one of the safest methods for producing data with high spatial resolution, and it is also a low-risk, non-invasive modality [1]. MRI, which is also considered an advanced imaging technique, provides structural and anatomical information on the human brain as soft tissue [2]. Moreover, the human brain is the most complex organ in the human body, with an intricate anatomy that interfaces with almost all other organs through trillions of synapses. The brain includes many complicated regions, including the basal ganglia and cerebellum. The supratentorial cortex is divided into four paired lobes: frontal, parietal, temporal, and occipital. The brain stem, located between the spinal cord and the rest of the brain, controls breathing and sleep. The frontal lobe manages problem solving, judgement and motor function, while the parietal lobe manages body position, hand writing, and sensation. The temporal lobe is responsible for memory and hearing, and the occipital lobe processes visual signals [3]. The massive amount of 3D brain data collected through MRI technique requires segmentation for the purposes of further image analysis. In image processing and analysis, segmentation is the process of dividing or categorizing images into segments or blocks based on the mutual property specified according to which each region is to be extracted [4]. The fundamental process that facilitates image analysis, understanding, interpretation and recognition is image segmentation. Manual segmentation is a traditional approach that is still used in some cases, but it is a very challenging and time consuming method requiring a high level of precision and certain tools, and it sometimes yields non-reproducible results. Therefore, semi- or fully automatic segmentation algorithms are necessary to segment brain data. Primary methods of MRI brain segmentation are concentrated on clustering of the brain into three main classes: white matter (WM), grey matter (GM) and cerebrospinal fluid (CSF). Over the past two decades, segmentation of the whole brain into the primary cerebrum tissues (i.e. CSF, GM, and WM) has been one of the core challenges in neuroimaging, which is still an active area of research using novel techniques [5]. However, brain MRI segmentation (BMS) is challenging and requires several preprocessing steps due to low signal to noise ratio (SNR) and artifacts in raw MRI data. The main sources of noise are categorized as biological and scanner noises because of tissue non-uniformity and limitations in hardware [6]. Various segmentation techniques are utilized in BMS, including statistical, image intensity-based methods, which will be discussed later.

## **2. Concepts and Methods**

Understanding brain structure helps researchers to optimally develop models and algorithms for brain MRI segmentation. In addition, structural MRI data require certain preprocessing steps to remove noise and artifact from the data. Various neuroimaging scientists and researchers have developed or improved upon methods to overcome such challenges. These methods are basically categorized into three primary classes: boundary-based methods, region-based methods and hybrid methods. In boundary or edge-based methods, or techniques, the gradient or edge-based features surrounding an object boundary are used as a measure of discontinuity to assist in segmentation. In region-based methods, brain MR segmentation is usually performed through the identification of a homogeneity feature that signifies one of the corresponding brain tissues. Hybrid methods include a combination of similarity and discontinuity to segment images. In modern techniques, as well as those

techniques mentioned earlier, a decision-making algorithm can result in highly accurate segmentation [7,8,9].

## 2.1. Brain Structure

The central nervous system (CNS) is comprised of the brain and spinal cord. The brain is the most complex organ in the human body, controlling all activities. In one respect, the brain is made of three major parts: the forebrain, the midbrain and the hindbrain. MRI has the capability of imaging the three brain parts by acquiring data from different angles and producing 3D sMRI data. The forebrain consists of the cerebrum, thalamus and hypothalamus (part of the limbic system). The midbrain consists of the tectum and tegmentum. The hindbrain is comprised of the cerebellum, pons and medulla. Often the midbrain, pons, and medulla are referred to in combination as the brainstem. The cerebrum, or cortex, is the largest part of the human brain, associated with higher brain functions, such as thought and action. The cerebral cortex is divided into four sections, or lobes: the frontal lobe, parietal lobe, occipital lobe and temporal lobe. The frontal lobe is associated with reasoning, planning, parts of speech, movement, emotions and problem solving. The parietal lobe is associated with movement, orientation, recognition and perception of stimuli. The occipital lobe is associated with visual processing. The temporal lobe is associated with perception and recognition of auditory stimuli, memory and speech [3].

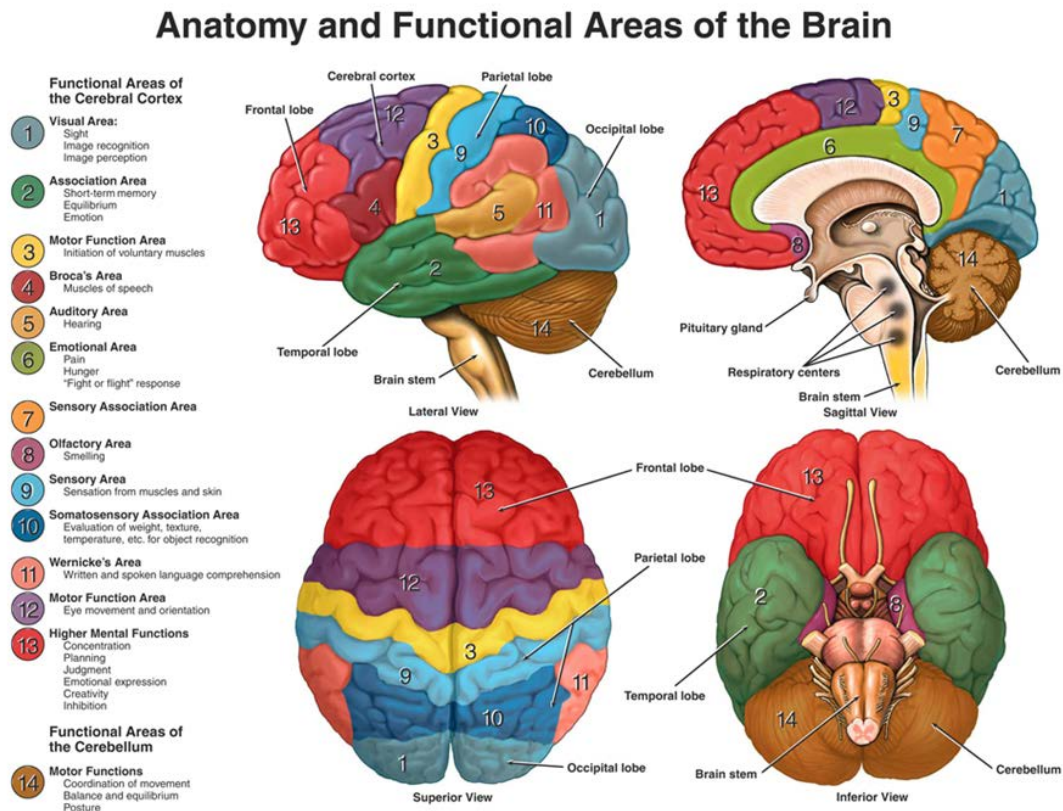


**Figure 1:** The brain regions and functions (Image courtesy: Animated Dissection of Anatomy for Medicine A.D.A.M. [www.adam.com](http://www.adam.com))

## **2.2. Brain Subcortical Structures**

The subcortical structures receive massively different inputs from the cerebral cortex and peripheral sense organs and stretch receptors. Through recurrent feedback loops, this information is integrated and shaped to provide output, which contributes to scaling, sequencing and timing of movement, as well as learning and automatization of motor and nonmotor behaviors. The cerebellum is the first subcortical structure, and in terms of functional neuroanatomy, the cerebellum can roughly be divided into (1) vestibulocerebellum integration of vestibular information, (2) spinocerebellum integration of sensory information from the body, and (3) pontocerebellum integration of information from the cortex regarding planned or ongoing movement. Its functionality is proposed as follows: (1) a timing device for movement, (2) facilitation of motor learning, and (3) facilitation and correct scaling and harmonization of muscle activity. Clinical features of cerebellar lesions include impairment of movement with dysmetria ('past-pointing'), dysdiadochokinesia, truncal and gait ataxia (in midline vermal lesions), dysarthria, and abnormal eye movements (commonly nystagmus).

The second brain subcortical structure is the Basal ganglia, and from the perspective of functional neuroanatomy, they participate in multiple parallel loops that transfer information from different (mainly cortical) areas and in turn transfer feedback (primarily) to those same areas. Input is mainly from the striatum; output comes almost exclusively from either the globus pallidus interna or the substantia nigra pars reticulata, which send inhibitory projections to the thalamus. Dopamine is the main neurotransmitter that regulates activity. The thalamus function includes four main roles, which are as follows: (1) release of desired movement from inhibitory control, (2) inhibition of undesired movement, (3) facilitation of sequential automatic movements, and (4) integration of attentional, reward and emotional information into movement and learning. Clinical features of basal ganglia lesions include rigidity, akinesia, and dystonia.

The thalamus is the third subcortical part of the human brain. In functional neuroanatomy, the thalamus receives afferent input from the special senses, basal ganglia, cerebellum, and cortex and brainstem reticular formation. Efferent output is primarily directed to the cortical areas and striatum. The main thalamic functions are thought to include: (1) modulation of sensory information by integration of brainstem (in particular the reticular activating complex) and relevant cortical information; and (2) modulation of cortical activity via cortico-thalamocortical loops. Clinical features of thalamic lesions include: (1) sensory abnormalities ranging from loss to deep-seated, severe pain; (2) motor disorders, e.g., hemiplegia; and (3) movement abnormalities, e.g. myoclonus and dystonia, usually in the context of lesions that also involve the basal ganglia [3].

## **2.3. MRI and Preprocessing**

The intensity of brain tissue is one of the most important features of brain MRI segmentation. However, when intensity values are affected by MRI artifacts, such as image noise, partial volume effect (PVE), and bias field effect, intensity-based segmentation techniques can lead to inaccurate results. Consequently, to obtain relevant and accurate segmentation results, several preprocessing steps are required to prepare MRI data. For example, it is essential to remove background voxels, extract brain tissue, perform image registration for multimodal segmentation, and remove the bias field effect. When the bias field, non-brain structures (e.g., the skull and the

scalp) and background voxels are removed, the histogram of the human brain MRI has three main peaks, which correspond to the three main tissue classes. In the healthy adult brain, the intensity variation within tissue is small, and the intensities inside the brain can be considered to be a piecewise constant intensity function, corrupted by noise and PVE. The PVE describes the loss of small tissue regions due to the limited resolution of the MRI scanner. This means that one pixel/voxel lies in the interface between two (or more) classes and is a mix of different tissues. This problem is even more critical in imaging of the small neonatal brain. The correction of PVE will be addressed in Section 4.6. It has been shown that the noise in the magnitude images is governed by a Rician distribution, based on the assumption that the noise on the real and imaginary channels is Gaussian. The probability density function for a Rician distribution is defined as follows:

$$f_{Rice}(x) = \frac{x}{\sigma^2} \exp\left(-\frac{(x^2 + y^2)}{2\sigma^2}\right) I_0\left(\frac{xy}{\sigma^2}\right)$$

**Figure 5:** Rician distribution

Where  $x$  is the measured pixel/voxel intensity,  $v$  is the image pixel/voxel intensity in the absence of noise,  $\sigma$  is the standard deviation of the Gaussian noise in the real and the imaginary images, and  $I_0$  is the zero order modified Bessel function of the first kind.

As mentioned above, several preprocessing steps are required to clean MRI data from noise or artefacts. However, the preprocessing steps vary in different studies. The most effective and popular processing steps are as follows:

Geometric distortion derives from various sources, such as nonlinear gradient magnetic field, or susceptibility and chemical shift. Using standard phantoms, this distortion can be corrected.

Intensity non-uniformity is primarily caused by inhomogeneity in the main magnetic field. Additionally, gradient inhomogeneity, radiofrequency inhomogeneity, amplifiers and analog-to-digital converters can cause this issue. To correct intensity non-uniformity, the bias field is estimated.

Noise reduction is often corrected through applying certain image processing techniques such as blurring, anisotropic blurring or a non-local means filter. For instance, spatial smoothing using a Gaussian filter is performed to remove noise from structural MRI data.

Motion correction is one of the most important steps in the preprocessing of MRI data. Because of any unexpected patient movement, an MRI slice can be affected. This can be corrected through the inter-session or intra-contract corrections method.

Skull stripping is the process of finding the skull region in the brain and removing that region from each MRI slice. As mentioned earlier, the ultimate goal of brain segmentation is to classify the brain into three major classes, or additional subclasses. Skull removal helps to analyze the meaningful regions of the brain that contain any structural or functional information.

Intensity normalization is a semi-optional step that depends on the type of analysis. Researchers sometimes perform normalization within an individual subject or on a global scale [7].

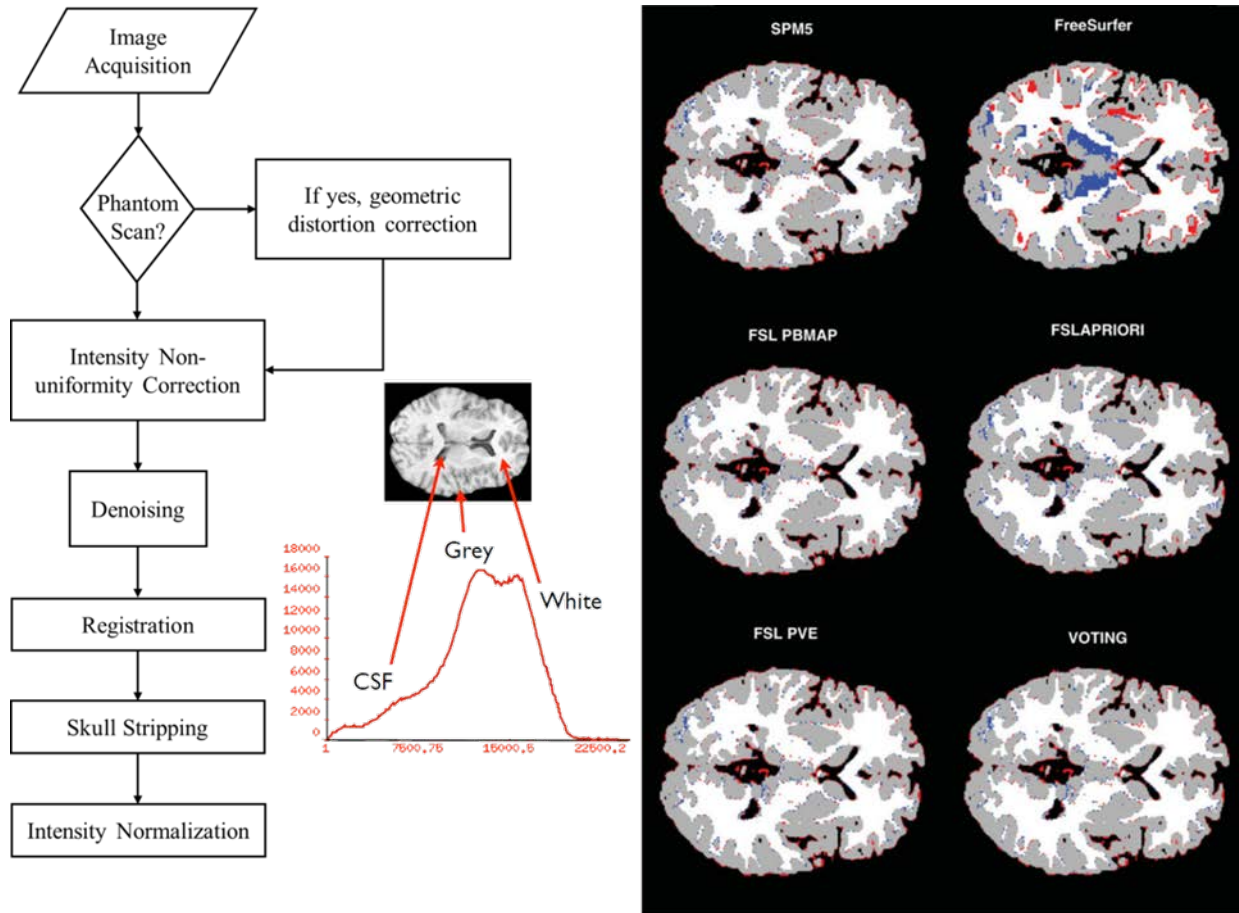


**Figure 2:** The left image shows the MRI data preprocessing pipeline. The middle image shows the histogram of a middle slice of MRI data. The right image shows six segmented brains (a middle slice) using different software packages such as FSL, SPM and FreeSurfer. The white regions represent White Matter, the grey regions represent Grey Matter and the black regions within the brains represent the CSF (Image courtesy: Dr. Andreas Meyer-Lindenberg).

#### 2.4. Segmentation Methods

Difficulties in brain MR image segmentation have led researchers to develop various image processing or machine learning-based algorithms to segment the brain into WM, GM and CSF, or to further segment the brain into subregions. However, due to complexity of this segmentation task, novel methods have been developed by combining certain techniques followed by decision-making algorithms [8]. In general, the BMS is categorized as follows:

- manual segmentation;

- intensity-based methods, including thresholding, region growing, classification and clustering;
- atlas-based methods;
- surface-based methods, including active contours and surfaces, and multiphase active contours
- hybrid methods.

#### **2.4.1. Manual Segmentation**

This classic technique refers to the segmentation process in which a human being who is usually an expert physician, neuroscientist or individual who knows and understands brain anatomy labels the brain regions by using basic brain imaging software tools. This slice-by-slice segmentation method can be the most accurate method, but it is very time-consuming and might be non-reproducible if it is done by a non-expert. Manual segmentation is often done and is still used to define a surrogate for true delineation and to prepare ground truths and labels to validate other segmentation techniques. For manual segmentation, editing software packages such as ITK-SNAP (<http://www.itksnap.org>) usually display 3D data in the form of three synchronized 2D orthogonal views (sagittal, coronal, and axial), onto which the operator draws the contour of the target structure. The output data therefore consists of a series of 2D contours, from which a continuous 3D surface must be extracted. This is a nontrivial post-processing task that is prone to error. For instance, due to inter-slice inconsistencies in segmentation, bumps in the reconstructed 3D surface are inevitable. More robust segmentation methods can usually be derived from true 3D structural models because they can globally ensure smoother and more coherent surfaces across slices.

#### **2.5. Intensity-based Methods**

In this category, segmentation methods classify brain regions directly based on pixel or voxel image intensity, or indirectly through image intensity-based features extracted from brain images. Although these methods are the most popular and straightforward techniques, their application is limited to three brain region classifications. Due to the high correlation of image intensities within WM, GM and CSF tissues, a detailed and subregional classification is highly challenging and often fails. Moreover, the classification of WM and GM may sometimes fail if the SNR of data is still low after preprocessing.

##### **2.5.1. Thresholding**

A histogram of a given brain slice, as shown in Figure 2, indicates certain peaks representing the main three regions in the brain. Thresholding the histogram is a straightforward way to segment the brain. In this technique, the algorithm attempts to determine the optimal intensity values for each peak and sometimes a meaningful interval for the optimal value called threshold  $\tau$  to segment the three brain regions. Thresholding methods have many variations: global (single threshold) or local threshold (depending on the position in the image), multi-thresholding, adaptive thresholding, and so forth. The following Figure demonstrates how the thresholding method applies to a brain image of  $I(i, j)$  to segment the three regions.

$$I_{tr} = \begin{cases} GM, & \text{if } \tau_1 - \sigma < I(i, j) < \tau_1 + \sigma \\ WM, & \text{if } \tau_2 - \delta < I(i, j) < \tau_2 + \delta \\ CSF, & \text{otherwise} \end{cases}$$

**Figure 6:** Thresholding algorithms to segment the brain into three regions.

Where  $I_{tr}$  represents the segmented regions,  $\tau_s$  are thresholds extracted from the image histogram and  $\sigma, \delta$  are an interval estimate that also must be calculated based on the histogram. Finding the best thresholds and interval values are data dependent processes that vary according to the data. However, using grid search or greedy algorithms, optimal values are obtained. The extant research has shown that an identical form of MR preprocessing, including image normalization, can achieve similar thresholds and intervals in different datasets.

Thresholding is a simple and computationally efficient technique, but it does not consider spatial characteristics of an image, such as neighborhood data. However, the thresholding method has limitations since it is sensitive to noise and intensity inhomogeneity. In low-contrast and poor resolution images, this technique fails to properly segment the brain, producing scattered labels instead of connected blobs, and it may require connectivity algorithms as a post-processing step. In general, threshold-based segmentation methods are not suitable for textured images. This is because the perceptual qualities of textured images are based on higher-order interactions between image elements or objects in the scene. However, in brain MRI segmentation, thresholding can be used to separate background voxels from brain tissue or to initialize the tissue classes in iterative segmentation methods.

### 2.5.2. Region Growing

A region growing algorithm is a simple segmentation method that merges pixels based on certain criteria. This method, which is also called “region merging,” attempts to consolidate juxtaposed pixels and create a blob or region based on similarities such as image intensity. In other words, this technique is used for extracting a connected region of the image consisting of groups of pixels with similar metrics (i.e., intensities). In its simplest form, region growing starts with a seed point (pixel/voxel) that belongs to the object of interest. The seed point can be manually selected by an operator or automatically initialized with a seed-finding algorithm. Region growing then examines all neighboring pixels/voxels, and if their intensities are sufficiently similar (satisfying a predefined uniformity or homogeneity criterion); they are added to the growing region. This procedure is repeated until no more pixels/voxels can be added to the region. Region growing is appropriate for segmentation of volumetric images that are composed of large connected homogeneous regions. Accordingly, it is successfully used in medical image analysis to segment different tissues, organs, or lesions from MR images. The main drawback of the region growing technique is its sensitivity to the initialization of the seed point. By selecting a different seed point, the segmentation result can be completely different. If seed point and homogeneity criterion are not properly defined, the growing region can leak out and merge with the regions that do not belong to the object of interest. Region growing is also sensitive to noise, and as a result, segmented regions in the presence of noise can become disconnected.



### 2.5.3. Machine Learning Methods

Machine learning techniques are categorized into supervised and unsupervised learning. In supervised methods, a model or algorithm is trained using training samples while the ground truths and labels are provided for each sample. In unsupervised methods, no label is provided for samples, and the term “unsupervised” refers to data without ground truth. Both supervised and unsupervised methods are used in BMS, but unsupervised methods have been of greater interest to researchers. As mentioned in the BM manual segmentation section, preparing labels for training samples requires significant efforts. On the other hand, most supervised learning methods require numerous samples in the training phase. Therefore, providing enough samples to successfully train a classifier is challenging. In contrast, unsupervised techniques are less sensitive to data size and can function even in the case of small data size. However, the accuracy of classification might not be as good as supervised methods, but it can compete in certain cases.

**K-nearest-neighbor (K-NN)** is a simple and supervised classifier which divides the brain into blocks based on the closest distance (image intensity). The KNN classifier is considered a nonparametric classifier because it makes no underlying assumption about the statistical structure of the data. Segmentation is then calculated in an iterative process by interleaving the segmentation refinement while updating the non-rigid alignment to the template. This procedure requires manual selection of a large number of training samples for each tissue class to train the KNN classifier. Due to the manual interaction in the training phase, the method is not fully automatic, and the results depend on the particular choice of the training set.

The **Bayesian**, or the naïve Bayes classifier, is a probabilistic classifier based on Bayes’ theorem with naïve independence assumptions between features. In simple terms, Bayesian probability is represented as follows:

$$\text{posterior} = \frac{\text{prior} \times \text{likelihood}}{\text{evidence}}$$

**Figure 7:** Bayesian probability

Bayesian classifiers are used in expectation-maximization (EM) segmentation methods, which have been successfully implemented in several software packages used in the medical imaging community: SPM, FAST, FreeSurfer, and 3DSlicer. All of these methods implement segmentation and bias correction in the EM framework.

**Artificial Neural Network (ANN)** and Support Vector Machines (SVM) are more complicated supervised learning techniques where decent amounts of training data are required. Due to the high complexity of those models, there is the potential for under- or overfitting of the models. Additionally, the provision of training data is always challenging. However, they yield a very high accuracy rate for classification once the training process is successfully performed.

The **Hidden Markov Random Field (HMRF)** model is derived from hidden Markov models (HMM), which are defined as stochastic processes generated by a Markov chain whose state/sequence cannot be observed

directly, but through a sequence of observations. Each observation is assumed to be a stochastic function of the state, or sequence. The underlying Markov chain changes its state according to a transition probability matrix, which is the number of states. HMMs have been successfully applied to speech recognition and handwritten script recognition. Since original HMMs were designed as one-dimensional (1-D) Markov chains with first-order neighborhood systems, they cannot be directly used in two-dimensional (2-D)/3-D problems such as image segmentation. Here, we consider a special case of an HMM in which the underlying stochastic process is an MRF instead of a Markov chain and is therefore not restricted to one dimension. An FSL FAST software package has been developed based on this algorithm, and its classification results have been very satisfying over the past several years [2].

**Clustering** methods are unsupervised learning algorithms. Unlike classification methods, no labels are provided in the clustering (segmentation) process. Most of the clustering methods aim to group samples (pixels) based on a given distance definition. These methods are broadly used to segment the brain into the three main regions. The most commonly used clustering methods are k-means clustering, fuzzy c-means clustering, and the expectation-maximization method (EM).

In the **k-means** clustering method, which is the most popular unsupervised learning algorithm and has successfully solved various clustering problems, the samples (pixels) are categorized based on fixed apriori knowledge, which is the number of cluster (K). The main idea is to define k centers, with one for each cluster. These centers are strategically placed, because different locations cause different results. Therefore, the better choice is to place them as far away from each other as possible. The next step is to take each point belonging to a given data set and associate it to the nearest center. When no point is pending, the first step is completed, and an early group age is done. At this point, we need to re-calculate k new centroids as the barycenter of the clusters resulting from the previous step. After these k new centroids are defended, a new binding is performed between the same data set points and the nearest new center using a loop that is already generated. As a result of this loop, the k centers may change their location step by step until no more changes are required or, in other words, the centers do not move any more. Finally, this algorithm aims at minimizing an objective function known as the squared error function, which is given by:

$$J = \sum_{j=1}^k \sum_{i=1}^n \|x_i^{(j)} - c_j\|^2$$

**Figure 8:** K-Mean SSE function

Where k is the number of clusters, n is the number of samples, and  $c_j$  is a given centroid. Additionally,  $\|x_i^{(j)} - c_j\|^2$  is a chosen distance measure between a given data point and cluster center. In more complicated cases, instead of Euclidian, the Mahalanobis distance is calculated. This distance is a multi-dimensional generalization for measuring how many standard deviations away  $x_i^{(j)}$  is from the mean of  $c_j$ .

The **fuzzy c-means (FCM)** algorithm is an unsupervised clustering method that allows one sample (pixel) to

belong to more than one cluster. FCM partitions a set of  $n$  objects  $x = \{x_1, x_2, \dots, x_n\}$  in  $R^d$  dimensional space into  $c$  ( $1 < c < n$ ) fuzzy clusters with  $y = \{y_1, y_2, \dots, y_c\}$  cluster centers or centroids. The fuzzy clustering of objects is described by a fuzzy matrix  $\mu$  with  $n$  rows and  $c$  columns in which  $n$  is the number of data objects and  $c$  is the number of clusters.  $\mu_{ij}$ , the element in the  $i^{\text{th}}$  row and  $j^{\text{th}}$  column in  $\mu$ , indicates the degree of association or membership function of the  $i^{\text{th}}$  object with the  $j^{\text{th}}$  cluster. The objective function of the FCM algorithm is to minimize the following Figure:

$$J_m = \sum_{j=1}^c \sum_{i=1}^n u_{ij}^m d_{ij}$$

$$d_{ij} = \|x_i - y_j\|$$

**Figure 9:** FCM objective functions

Where  $n$  is the number of image elements that need to be partitioned into  $c$  clusters,  $u_{ij}$  is the membership function of the element  $x_j$  (a feature vector at position  $j$ ) belonging to the  $i^{\text{th}}$  cluster,  $m$  is the weighting exponent that controls the fuzziness of the resulting partition (most often is set to  $m = 2$ , if  $m = 1$  we have the k-means clustering), and  $d_{ij}$  is the similarity measure between  $x_j$  and the  $i^{\text{th}}$  cluster center  $y_j$ . The FCM algorithm iteratively optimizes  $J_m$  until the stop criterion is satisfied. The FCM process is summarized as follows [9] [10]:

- Select  $m$  ( $m > 1$ ); initialize the membership function values  $\mu_{ij}, i = 1, 2, \dots, n; j = 1, 2, \dots, c$ .
- Compute the cluster centers  $y_j, j = 1, 2, \dots, c$
- Compute the Euclidian distance  $d_{ij}, i = 1, 2, \dots, n; j = 1, 2, \dots, c$ .

The expectation maximization (EM) method is an iterative method for finding the maximum likelihood or MAP estimates of a statistical model. It has the same soft classification principle as the FCM method but typically assumes that MRI intensities of different brain tissues can be represented with a Gaussian mixture model. Even though clustering methods do not require training images, they do require some initial parameters, and the EM method has shown the highest sensitivity to initialization in comparison to FCM and k-means methods [8]. Figure 3 shows the results of WM, GM and CSF segmentation using k-means clustering.

## 2.6. Atlas-based Methods

Certain research groups have developed brain atlases, including three main regions and subregions. The atlases are probability maps indicating where each voxel is associated to which region in the brain based on what probability. This brain segmentation method is one of the most accurate approaches if the atlases are available. The Harvard-Oxford cortical and subcortical structural atlases, Jülich histological (cyto- and myelo-architectonic) atlas, JHU DTI-based white-matter atlases, Oxford thalamic connectivity atlas, Oxford-GSK-Imanova structural and connectivity striatal atlases, Talairach atlas, MNI structural atlas, probabilistic cerebellar

atlas from UCL, subthalamic nucleus atlas from the Cognitive Science Center Amsterdam at University of Amsterdam, connectivity-based parcellation atlases and automated anatomical labeling (AAL, or anatomical automatic labeling) atlases are the most popular atlases developed by famous research groups across the world. It is worth mentioning that most of the atlases have been developed using healthy control brain data for a certain age range. In order to use a standard atlas, image registration techniques are required to align the brain MR data with the standard atlas. Image registration is often challenging, especially when the brain data have been collected from clinical subjects (such as Alzheimer's or Parkinson's patients) or from older adults. Differences in age range and type of brain disorder cause failures in image registration, which restricts the use of a standard atlas in the segmentation of brain images. Figure 4 [11] illustrates brain parcellation using different atlases.

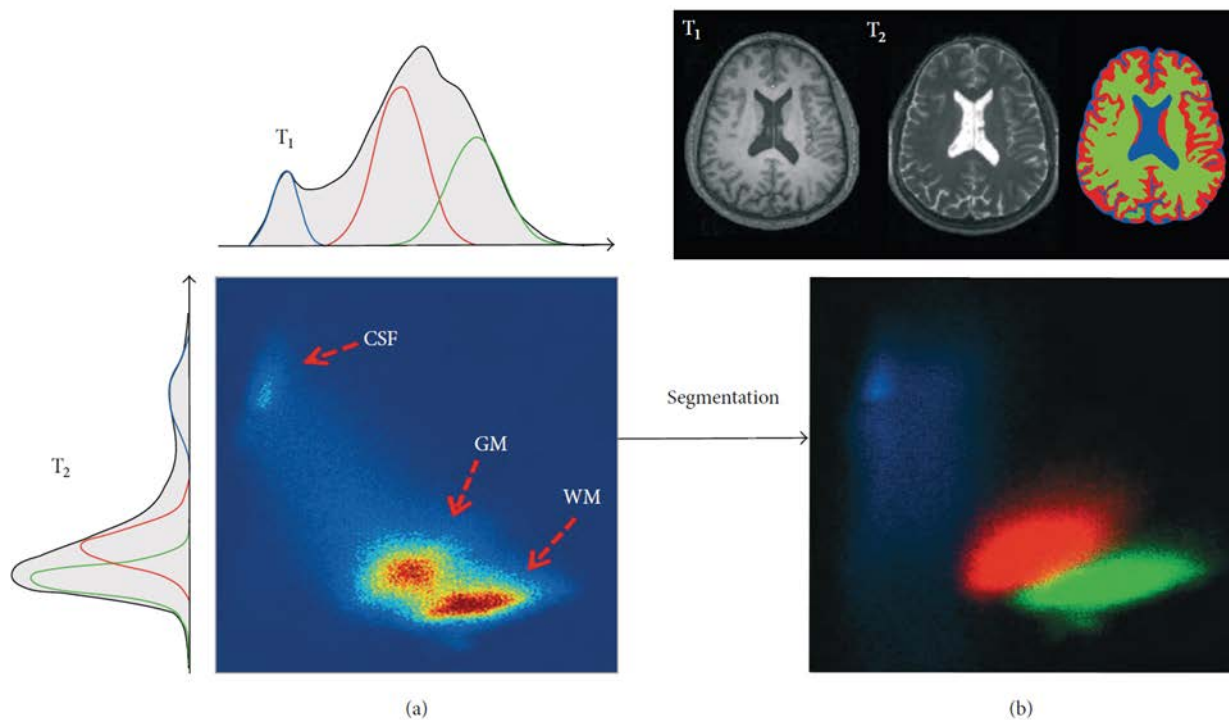


**Figure 3:** (a) Joint 2D intensity histogram of T1-W and T2-W MRI of the adult brain. The associated 1D histograms of each MRI modality are plotted on the left and top. Both individual histograms consist of three overlapping Gaussian distributions that approximate the expected tissue distribution of GM, WM and CSF. (b) The scatter plot of the tissues intensities after applying tissue segmentation. The horizontal axis represents T1-W intensities and the vertical axis represents T2-W intensities. The red cloud corresponds to GM, the green to WM, and the blue to CSF.

### 2.7. Surface-based Methods

In the surface-based segmentation algorithm, every connected region of pixels of a given type is eroded (contracted) until a sufficiently small number of pixels are obtained in the largest connected subregion. This region serves as the seed region to an iterative region growing algorithm based on fitting variable order surfaces to the original image data in the seed region and subsequent growth regions. The iterative region growing process is directly controlled by (1) the surface fit error obtained at any iteration (2) a pre-specified error

tolerance, and (3) a regions test, which is a generalization of the one-dimensional runs test of nonparametric statistics for regression analysis. The iteration continues until the termination criteria are met, at which point the computed surface region description is rejected or accepted [12]. These approaches include surface-based methods, such as deformable models including active contours and surfaces.

### ***2.7.1. Active Contours and Surfaces***

The term “deformable model” (DM) was pioneered by Terzopoulos et al. to refer to curves or surfaces, as defined in the image domain, which are deformed under the influence of internal and external forces. Internal forces are connected with the curve features and strive to keep the model smooth during the deformation process. On the other hand, external forces are responsible for attracting the model toward features of the structure of interest, and are connected with the image features of the adjacent regions to the curve. Hence, DM tackles the segmentation problem by considering an object boundary as a single, connected structure, and exploiting a priori knowledge of object shape and inherent smoothness. Although DMs were originally developed to provide solutions for computer vision applications to natural scenes and computer graphics problems, their applicability in medical image segmentation has already been proven. Deformable models use closed parametric curves or surfaces for delineating region boundaries. The parametric curves and surfaces deform under the influence of external (or image) forces (controlled by image attributes) and internal forces that control surface regularity. In general, deformable models represent the fusion of geometry, physics, and the approximation theory. Geometry is used to represent the shape of the object, physics defines constraints on how the shape may vary over time and space, and the approximation theory provides mechanisms for fitting the models to measured data.

### ***2.8. Hybrid Segmentation Methods***

Hybrid segmentation methods are novel segmentation approaches in which more than one strategy is used to segment the human brain into the three main regions or into subregions. As explained before, using one method for brain MR image segmentation does not usually yield the highest accuracy rate. Therefore, hybrid or combined segmentation methods have been used extensively in different brain MRI segmentation applications. The main idea is to combine different complementary segmentation methods into a hybrid approach to avoid many of the disadvantages of each method alone and to improve segmentation accuracy. The simplest method is to utilize one of the clustering methods mentioned earlier, followed by a decision-making algorithm in order to decrease false positive rates. Kapur et al. segmented different brain regions in adults using 2D MRI through combining expectation maximization segmentation, dual mathematical morphology, and active contour models. Masutani et al. developed a combined model-based region growing algorithm with morphological information of local shape to segment cerebral blood vessels. Warfield et al. combined a 3D brain MRI parcellation method that iterates between a classification step to identify regions and an elastic matching step to align a template of normal brain anatomy with the classified regions. Moreover, an unsupervised global-to-local brain MRI segmentation has been developed by Xue et al., in which a minimum error global thresholding approach and a spatial-feature based on fuzzy c-means clustering approach were merged to segment 3D MRI at the slice level. Vijayakumar and Gharpure developed a hybrid MRI segmentation algorithm using artificial neural networks

(ANN), and they also suggested the method for segmenting tumor lesions, edema, cysts, necrosis, and normal tissue in T2 and FLAIR MRI. More recently, Ortiz et al. suggested an improved brain MRI segmentation method using self-organizing maps (a particular case of ANN) and entropy-gradient clustering.

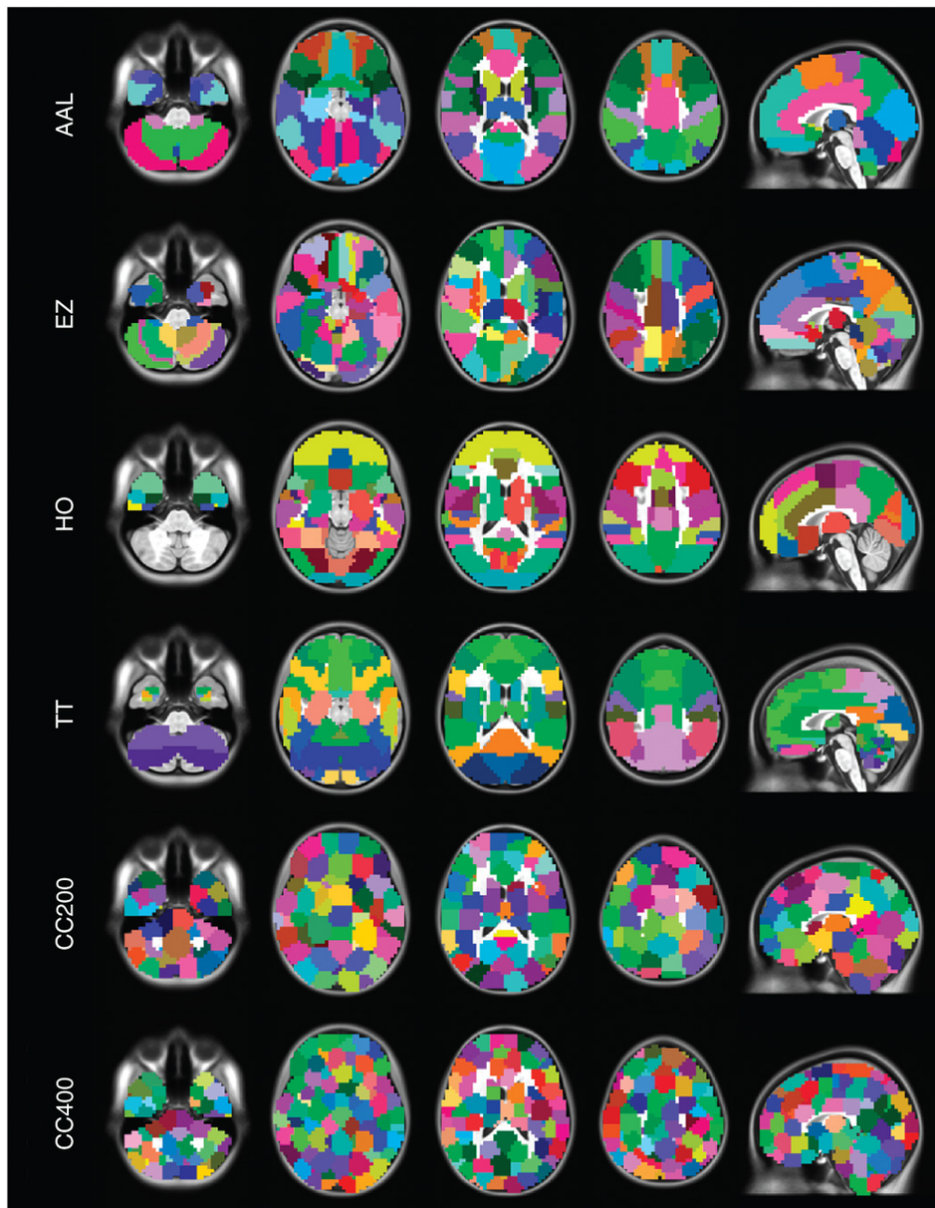


**Figure 4:** Atlases of brain areas generated using anatomical (top four rows) and functional (bottom two rows) parcellation schemes show a lateral view (right) and top views of the human brain. AAL (automated anatomical labeling) and Harvard Oxford (HO) are derived from anatomical landmarks (sulci and gyral). The EZ (Eickhoff–Zilles) and TT (Talariach Daemon) atlases are derived from postmortem cyto- and myelo-architectonic segmentations. The CC200 and CC400 atlases are derived from 200- and 400-unit functional parcellations.

### 3. Validation

The validation process is an important step that is required to define the reliability and reproducibility of a given brain MRI segmentation method. Similar to most validation techniques, the ground truth, or so-called labels, is required for data to validate the algorithm. The segmented brain images are compared to the corresponding ground truth, and most of the time, an accuracy rate as the validation metric is calculated. For instance, the number of pixels that have been correctly segmented is divided by the total number pixels in the brain. Another method is the Dice coefficient definition, which is used to quantify the overlap between the MRI segmentation and the given “ground truth,” defined as follows:

$$\text{Dice Coefficient}_i = \frac{2|A_i \cap B_i|}{|A_i| + |B_i|}$$

**Figure 10:** Dice coefficient definition

Where  $i$  stands for a region type,  $A_i$  and  $B_i$  denote the set of pixels labeled into  $i$  by the “ground truth” and MRI segmentation, respectively, and  $|A_i|$  denotes the number of elements in  $A_i$ . The Dice coefficient is in the range  $0 \leq \text{Dice Coefficient}_i \leq 1$  and has a value of 0 if there is no overlap between the two segmentations and 1 if both segmentations are identical.

### 4. Conclusion

The segmentation of brain MR images is an important but challenging step in medical image analysis in both clinical and research areas. From 3D MRI data visualization to structural MR data analysis, brain segmentation represents an essential step in the process. Various techniques, such as threshold-based, machine learning-based or hybrid methods, have been developed and optimized to perform brain parcellation. However, not all techniques produce a high accuracy rate, which is due to a variety of issues. For instance, supervised machine learning methods require enough labeled data (ground truth) to train a model than can segment the brain with a high accuracy rate. As mentioned above, providing the ground truth by manually segmenting the data is a time-consuming approach. Consequently, unsupervised machine learning using unsupervised methods, or so-called clustering algorithms, are of greater interest. The extant literature reveals that several successful segmentation cases in which fuzzy c-means (FCM) was utilized have been reported. Furthermore, researchers have indicated that by combining various methods to develop hybrid algorithms, they have achieved more robust segmentation methods that yield higher accuracy rates.

### 5. Conflict of Interests

The authors declare that there is no conflict of interests regarding the publication of this paper.

## Reference

- [1] Si-Yuan Lu, Xing-Xing Zhou, Guang-Shuai Zhang, and Ling Wei., "A Short Survey on MRI Brain Detection," 2015.
- [2] Yongyue Zhang, Michael Brady, and Stephen Smith, "Segmentation of brain MR images through a hidden Markov random field model and the expectation-maximization algorithm," *IEEE transactions on medical imaging* , vol. 20, no. no. 1 , pp. 45-57, 2001.
- [3] Saman Sarraf, Jian Sun, "ADVANCES IN FUNCTIONAL BRAIN IMAGING: A COMPREHENSIVE SURVEY FOR ENGINEERS AND PHYSICAL SCIENTISTS," *International Journal of Advanced Research* , vol. 4, no. no. 8 , p. 640–660, August 31, 2016.
- [4] Reshma Hiralal, Hema P. Menon, "A Survey of Brain MRI Image Segmentation Methods and the Issues Involved," *In The International Symposium on Intelligent Systems Technologies and Applications*, pp. 245-259, 2016.
- [5] J. Dolz, L. Massotier, M. Vermandel, "Segmentation algorithms of subcortical brain structures on MRI for radiotherapy and radiosurgery: a survey," *IRBM* , vol. 36, no. no. 4, pp. 200-212, 2015 .
- [6] Jamal Ghasemi, Reza Ghaderi, MR Karami Mollaei, S. A. Hojjatoleslami, "A novel fuzzy Dempster–Shafer inference system for brain MRI segmentation," *Information Sciences* , vol. 223, pp. 205-220, 2013.
- [7] Saman Sarraf, Cristina Saverino, Halleh Ghaderi, John Anderson, "Brain network extraction from probabilistic ICA using functional Magnetic Resonance Images and advanced template matching techniques," in *Electrical and Computer Engineering (CCECE), 2014 IEEE 27th Canadian Conference*, Toronto, 2014.
- [8] Saman Sarraf , Cristina Saverino, Ali Mohammad Golestani, "A Robust and Adaptive Decision-Making Algorithm for Detecting Brain Networks Using Functional MRI within the Spatial and Frequency Domain," in *The IEEE International Conference on Biomedical and Health Informatics (BHI)* , Las Vegas, 2016.
- [9] S. Sarraf, "Hair Color Classification in Face Recognition using Machine Learning Algorithms," *American Scientific Research Journal for Engineering, Technology, and Sciences (ASRJETS)*, vol. 26, no. 3, p. 426, 2016.
- [10] S. Smith., "Fast robust automated brain extraction," *Human Brain Mapping*, vol. 17(3), no. November 2002, pp. 143-155, 2002.
- [11] Ivana Despotović, Bart Goossens, Wilfried Philips, "MRI segmentation of the human brain: challenges, methods, and applications," *Computational and mathematical methods in medicine*, 2015.
- [12] Mahesh Yambal, Hitesh Gupta, "Image segmentation using fuzzy C means clustering: a survey," *International Journal of Advanced Research in Computer and Communication Engineering* , vol. 2, no. no. 7, 2013.
- [13] Ivana Despotović, Bart Goossens, Ewout Vansteenkiste, Wilfried Philips, "An improved fuzzy clustering approach for image segmentation," in *In 2010 IEEE International Conference on Image Processing*, pp. 249-252. *IEEE*, 2010.



- [14] R. CameronCraddock, Saad Jbabdi, Chao-Gan Yan, Joshua T. Vogelstein, F. Xavier Castellanos, Adriana Di Martino, Clare Kelly, Keith Heberlein, Stan Colcombe, and Michael P. Milham, "Imaging human connectomes at the macroscale," *Nature methods* (2013): ., vol. 10, no. no. 6, pp. 524-539, 2013.
- [15] Paul Bed, Ramesh Jain, "Segmentation through symbolic surface descriptions," The University of Michigan, 1986.
- [16] Saman Sarraf, Ghassem Tofighi, "Deep Learning-based Pipeline to Recognize Alzheimer's Disease using fMRI Data," *bioRxiv*, vol. 066910, 2016.
- [17] Saman Sarraf, John Anderson, Ghassem Tofighi, "DeepAD: Alzheimer' s Disease Classification via Deep Convolutional Neural Networks using MRI and fMRI," *bioRxiv*, vol. 070441, 2016.